ISSN 1674-1056
http://cpb.iphy.ac.cn
http://iopscience.iop.org/cpb
中国物理 B
Chinese Physics
中国物理 Chinese Physics B

Dynamics of the $CH_4+O(^3P)\rightarrow CH_3(v=0)+OH(v'=0)$ reaction

Zhong-An Jiang(蒋仲安), Ya Peng(彭亚), Ju-Shi Chen(陈举师), Gui Lan(兰桂), Hao-Yu Lin(林浩宇)
Citation: Chin. Phys. B . 2018, 27(6): 063401. **doi:** 10.1088/1674-1056/27/6/063401

Journal homepage: http://cpb.iphy.ac.cn; http://iopscience.iop.org/cpb

What follows is a list of articles you may be interested in

Intrinsic product polarization and branch ratio in the$S(^1D, ^3P)+HD$ reaction on three electronic states

Lin Li(李琳), Shunle Dong(董顺乐)
Chin. Phys. B . 2016, 25(9): 093401. **doi:** 10.1088/1674-1056/25/9/093401

Quasi-classical trajectory study of collision energy effect on the stereodynamics of H + BrO→O + HBr reaction

Xie Ting-Xian, Zhang Ying-Ying, Shi Ying, Li Ze-Rui, Jin Ming-Xing
Chin. Phys. B . 2015, 24(4): 043402. **doi:** 10.1088/1674-1056/24/4/043402

Theoretical study of stereodynamics for the $N+H_2/D_2/T_2$ reactions

Li Yong-Qing, Zhao Jin-Feng, Zhang Yong-Jia, Chi Xiao-Lin, Ding Yong, Ma Feng-Cai
Chin. Phys. B . 2014, 23(12): 123401. **doi:** 10.1088/1674-1056/23/12/123401

Quasi-classical trajectory investigation on the stereodynamics of Li+DF (v=1-6, j=0)→LiF+D reaction

Zhang Ying-Ying, Li Shu-Juan, Shi Ying, Xie Ting-Xian, Jin Ming-Xing
Chin. Phys. B . 2014, 23(12): 123402. **doi:** 10.1088/1674-1056/23/12/123402

Quasi-classical trajectory study of the isotope effect on the stereodynamics in the reaction $H(^2S)+CH(X^2\Pi; v=0, j=1)\rightarrow C(^1D)+H_2(X^1\Sigma_g^+)$

Wang Yun-Hui, Xiao Chuan-Yun, Deng Kai-Ming, Lu Rui-Feng
Chin. Phys. B . 2014, 23(4): 043401. **doi:** 10.1088/1674-1056/23/4/043401

Dynamics of the $CH_4 + O(^3P) \rightarrow CH_3(v = 0) + OH(v' = 0)$ reaction*

Zhong-An Jiang(蒋仲安)†, Ya Peng(彭亚)‡, Ju-Shi Chen(陈举师), Gui Lan(兰桂), and Hao-Yu Lin(林浩宇)

School of Civil and Resource Engineering, University of Science and Technology Beijing, Beijing 100083, *China*

(Received 31 January 2018; revised manuscript received 4 April 2018; published online 10 May 2018)

The dynamics of the ground-state reaction of $CH_4 + O(^3P) \rightarrow CH_3(v = 0) + OH(v' = 0)$ have attracted a great deal of attention both theoretically and experimentally. This rapid communication represents extensive quasi-classical trajectory calculations of the vibrational distributions on a unique full-dimensional *ab initio* potential energy surface for the title reaction, at the collision energy of relevance to previous crossed molecular beam experiments. The surface is constructed using the all electrons coupled-cluster singles and doubles approach plus quasi-perturbative triple excitations with optimized basis sets. A modified Shepard interpolation method is also employed for the construction. Good agreement between our calculations and the available experimental results has been achieved, opening the door for accurate dynamics on this surface.

Keywords: quasi-classical trajectory calculation, vibrational distribution, product-scattering distribution, combustion reaction

PACS: 34.10.+x, 31.15.xv, 34.50.Lf **DOI:** 10.1088/1674-1056/27/6/063401

1. Introduction

Methane is the simplest organic fuel and the most abundant hydrocarbon in the atmosphere.[1–10] Representing an important initial step in methane combustion, the $CH_4 + O(^3P) \rightarrow CH_3(v = 0) + OH(v' = 0)$ reaction provides an ideal platform for studying bimolecular reactions involving one transfer of a hydrogen atom.[11–15] Over the last decade, experimental and theoretical studies on this reaction have greatly extended and advanced our understanding of chemical reaction dynamics.[16–21] Suzuki and co-workers measured the nascent v_2 out-of-plane bending vibrational distribution in the umbrella mode of CH_3 by an infrared diode laser absorption kinetic spectroscopy experiment, which suggested that the CH_3 moiety was gradually relaxed to a planar structure during these reactions.[22] Later Sweeney *et al.* measured the very low fractions of product rotational energy release for the higher homologues such as isobutane and cyclohexane by laser photolysis of NO_2 combined with laser-induced fluorescence detection of the nascent OH product.[16] The OH spin–orbit states were found to be nonstatistically populated, which was interpreted by a direct abstraction mechanism with a preferentially collinear C–H–O approach of the $O(^3P)$ atom to the C–H bond under attack. Moreover, a considerable body of work[23–26] was devoted to the experimental characterization of the OH molecule produced in related processes via molecular beams, like the reactions of the $O(^3P)$ atom with saturated, unsaturated aromatic hydrocarbons. Many correlated experiments on methane with H, F, Cl, and $O(^3P)$ have been reported after the first measurement of correlated angular and vibrational product distributions for the $F + CD_4$.[27]

Recently, there has been additional progress with a wide variety of methods, including the crossed beam technique, on the title reaction.[20,21,25,26,28] The internal energy distributions of products CH_3 and OH, as well as differential cross sections, were studied with isotopic variants taken into account to provide detailed information on product translational, vibrational energy distributions, and product angular distributions. The product speed distributions at different E_{col} were measured by a number of groups and the excitation functions were also obtained.[20,21] The reactions at center-of-mass collision energies in the range of 64.6 kcal/mol–89.9 kcal/mol were investigated with crossed-beams experiments and direct dynamics calculations, which provided evidence for the expected H–atom abstraction reaction.[20] This reaction was also studied at a hyperthermal collision energy of 64 kcal/mol by two crossed-molecular-beams techniques, in which the OH product was formed mainly from a stripping mechanism where the $O(^3P)$ reacts through large-impact-parameter collisions with CH_4. The CH_3 products are in the ground vibrational state, while the OH products are vibrationally cold and rotationally hot.[21] With extended collision energies ranging from 7.5 kcal/mol to 13.5 kcal/mol, it was revealed that the product angular distributions were backward scattered for the $O(^3P) + CHD_3$ reaction, which indicated a direct rebound mechanism. Liu and his co-worker measured the first differential cross sections, in which the first reported product angular distributions showed predominant backward scatterings for both ground-state and bend-excited methanes, indicating a

*Project supported by the National Natural Science Foundation of China (Grant Nos. 51574016 and 51604018).

†Corresponding author. E-mail: jza1963@263.net

‡Corresponding author. E-mail: pengyaustb@sina.com

© 2018 Chinese Physical Society and IOP Publishing Ltd

direct rebound reaction mechanism.[29] Later, they measured the reactive excitation function, as well as the product angular distributions and the energy disposal on initial collision energies, by taking images over the energy range of chemical significance.[21,25,26,28] These experimental results are a severe test for theoretical work on potential energy surface (PES) constructions and quasiclassical trajectory (QCT) calculations. The intersection angle of the two molecular beams was varied to investigate the initial translational energy dependence of the reactivity, thereby changing the relative collision energy in the center-of-mass frame. The ground state reaction producing $OH+CD_3$ has a threshold at 8.01 kcal/mol. Significant vibrational enhancement in the reaction rate was observed, and the product angular distribution shifted from a backward-dominance in $O(^3P)+CHD_3$ to a sideways-peaking upon CH stretching excitation.[25] Moreover,due to the focusing effects of the long-range anisotropic interactions en route to the barrier, vibrationally enhanced reactivity has also been observed in CHD_3 ($v_1 = 1$) by enlarging the cone of the reactive acceptance. Later, by imaging the effects of the antisymmetric-stretching excitation, it was found that the $OH(v' = 0)$ product was associated with a single peak, while the stretch-excited methane presented two peaks corresponding to the $OH(v' = 1)$ and $OH(v' = 1)$ states with populations 0.85:0.15 at $E_{col} = 12.4$ kcal/mol.[30] A reactive threshold at $E_{col} \approx 8$ kcal/mol was clearly discerned, which predicted the barrier height of 9 kcal/mol–10 kcal/mol. These quantitative results for the ground-state reaction provide a stringent test for further theoretical developments of the potential energy surface and dynamics calculations of this important polyatomic reaction.[25,30–32]

Theoretically, it has received a great deal of attention using various *ab initio* and dynamical methods.[33–37] Early in 1980, Walch and Dunning[33] studied the stationary points on the ground state PES with POL-CI wave functions. In 1990, Gonzalez *et al.* performed the geometry optimization of all stationary points including transition states in this reaction with the Hartree–Fock method.[34] The accurate dynamic investigation of the title reaction usually needs an accurate PES.[11,12,36,38–44] Until now, there have been several PESs constructed for the $O(^3P)+CH_4 \rightarrow OH+CH_3$ reaction, some QCT and reduced-dimensional quantum dynamics (QD) calculations have been performed using these PESs. The ground PES, constructed by Gonzáleza and co-authors[35] using the PMP4 calculations, were employed to obtain the barrier height of 13.3 kcal/mol and the zero-point-inclusive barrier height of 9.4 kcal/mol. Based on the information furnished by Joseph *et al.*[45] and Jordan *et al.*[46] for the $CH_4(X^1A_1)+H \rightarrow CH_3+H_2$ reaction, a 12-dimensional analytical PES was constructed[12,38] by making the previous one completely symmetric with respect to any permutation of the four methane hydrogens. In 2012, the high accuracy was achieved by using a large basis set and high-level electron correlation method to obtain the barrier height of 14.08 kcal/mol and the OHC bending angle of 179.3° at the saddle point, which was taken as a benchmark value.[40] In a recent study, a new full-dimensional analytical PES for $O(^3P)+CH_4$ was accurately constructed based on PES-2000 and further high level CCSD(T) = FULL/aug-cc-pVQZ *ab initio* data by González-Lavado and co-authors.[41] They concluded that the correlation of all electrons (FULL), including core and valence electrons, has a major influence on the description of the barrier. The barrier height obtained from this surface was 14.0 kcal/mol with the corresponding OHC bending angle of 180.0°. The title reaction, theoretically, has also received a great deal of attention using QCT calculations.[35,47,48] The mode-specific vibrational distributions were obtained by doing a normal-mode analysis, and the reaction was predicted to occur at small impact parameters and proceed through direct rebound pathways.[48] That the translational energy activates the reaction more efficiently than vibrational energy shows this central-barrier reaction behaves more like an early barrier reaction.

In the present study, we investigate the QCT calculations on the uniquely developed ground-state PES for the gas-phase $O(^3P)+CH_4 \rightarrow OH+CH_3$ reaction with the $^3A''$ transition state. The dynamical details of the title reaction are compared with the results of the universal crossed molecular beam experiments performed by Liu and his co-workers.[13,25,26,28,30]

2. Materials and methods

The ground PES for the gas-phase reaction of hydrogen-abstraction from methane by an oxygen atom has been performed using the all electrons coupled-cluster singles and doubles approach plus quasi-perturbative triples excitations. The *ab initio* calculations in the present work are conducted using the Gaussian 09 suite of *ab initio* programs.[49] The best compromise we could achieve was the all-electron coupled-cluster singles and doubles approach plus quasi-perturbative triples excitations, CCSD(T) (full), together with optimized aug-cc-pCVQZ basis sets. A reasonable consideration of the basis sets dependence is included. Several basis sets, including cc-pVXZ [X = D, T, Q, and 5], aug-cc-pCVXZ [X = D, T, and Q] and an optimized aug-cc-pCVQZ have been tested to obtain the reasonable barrier height and reaction endoergicity. Some results with previous reported calculations are presented schematically in Fig. 1, which illustrate the dramatic influence of electronic correlation and basis set on the reaction endoergicity (energy difference between $E_{Products}$ and

$E_{\text{Reactants}}$) with various *ab initio* calculations. The results of the all-electron calculation are generally better than those of the frozen-core. Basis set extensions from aug-cc-pCVDZ to aug-cc-pCVQZ decrease the barrier height (without zero-point-energy) by around 0.8 kcal/mol. To obtain the core and core-valence correlation effects on the energies, especially barriers,[41,50] the aug-cc-pCVQZ basis sets are chosen but optimized.[1] An optimized scheme was employed to adequately describe both core–core and core–valence correlations of the C/O atom.[51–53]

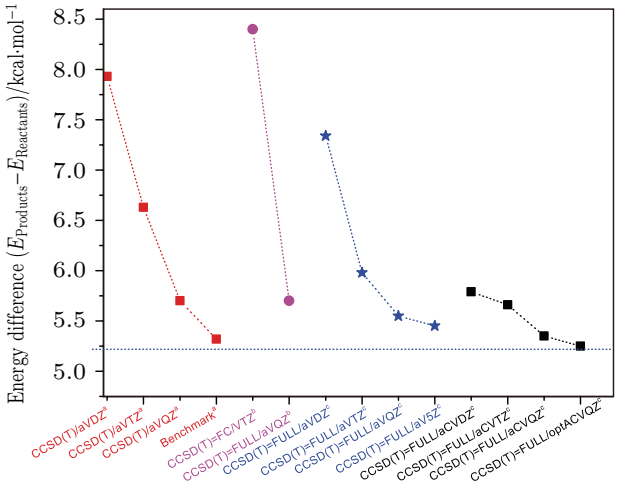


Fig. 1. (color online) The comparison of reaction endoergicity with various *ab initio* methods. a: CCSD(T)/aug-cc-pCVQZ calculations from Ref. [40]; b: the valence-electron CCSD(T)/(FC)cc-pVTZ level and the all-electron CCSD(T)/(FULL)aug-cc-pVQZ level from Ref. [41]; c: present work at the CCSD(T)=FULL/optACVQZ level. The energy of the $O(^3P)+CH_4(X^1A_1)$ asymptote is taken to be zero.

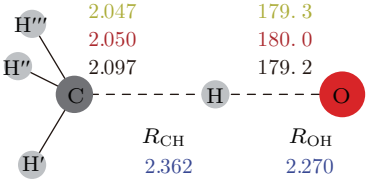
A modified Shepard interpolation method is employed for the construction of PES. This method was proposed by Collins and his co-workers[54–57] for systematically generating global *ab initio* PES for systems of more than four atoms. The PES is determined by the energies and the first and second order derivatives of the energy at a set of data point geometries.[54,55,58,59] Our interpolated PES in the present work for the reaction $O(^3P)+CH_4 \rightarrow OH+CH_3$ is grown from the initial set of 196 data points, and finally about 6100 data points are obtained. QCT calculations of the title reaction on the ground rovibrational state are performed using this new *ab initio* PES. The ability to perform classical dynamics simulations on multidimensional PES is limited in practice due to the exponential scaling with the number of nuclear degrees of freedom. The location of the data points is mainly determined using the iterative methods developed by Collins and his co-workers and the iterative development of the PES is implemented with the GROW package.[54,60,61] A set of geometries are chosen as an initial set of data points for GROW. These points should represent the chemically important regions in configuration space, typically the reactants, products, a saddle point, van der Waals potential wells and some configurations on a minimum energy path for the reaction. Additionally, some data points should be added according to physical considerations, particulary the analysis of potential contour plots.

3. Results and discussions

3.1. Accuracy of the PES

This new global 12-dimensional potential energy surface (denoted as PES-2017) using the methods described in the above for the gas-phase $O(^3P)+CH_4 \rightarrow OH+CH_3$ reaction is expected to give a better description of the regions around the transition state (TS), and of those long-range vdW interactions (reactant complex Well$_R$, Well$'_R$, and product complexes Well$_P$). The data point set is chosen mainly according to classical trajectory simulations. The geometrical structures of all reactants, transition state, complexes, and products are optimized at the CCSD(T) = FULL/optACVQZ level. This method was used to optimize geometrical structures of all stationary points calculations obtaining a good agreement with the experiments and our previous calculations.[1] The distance between two fragments of reactants/products is fixed at 30.0 bohr. At the same level, the corresponding frequency calculations of the optimized geometries are also performed to prove the character of minima without imaginary frequencies and the character of the transition state with only one imaginary frequency.

Parameter	$R_{CH''}$	$R_{CH'''}$	∠CHO
Corchado: 1998	2.033	2.033	180. 8
Troya: 2005	2.084	2.084	180. 0
Czako: 2012	2.047	2.047	179. 3
Gonzalez: 2014	2.050	2.050	180. 0
PES-2017	2.097	2.097	179. 2



Barrier	$R_{CH'}$	R_{CH}	R_{OH}
14. 0	2.033	2.362	2.270
14.37	2.084	2.338	2.328
14.08	2.047	2.434	2.292
14. 0	2.050	2.470	2.253
13.55	2.097	2.643	2.21 6

Fig. 2. (color online) Structural parameters (distances in bohr, angles in degrees and energies in units kcal/mol) for the transition state obtained from various *ab initio* levels. Corchado: geometry at the UMP2/cc-pVTZ level and energy at the PUMP2-SAC//UMP2/cc-pVTZ level from Ref. 38; Troya: PMP2/aug-cc-pVDZ from Ref. [19]; Czako: all-electron CCSD(T)/aug-cc-pCVQZ from Ref. [40]; Gonzalez: geometry at the valence-electron CCSD(T)/cc-pVTZ level and energy at the all-electron CCSD(T)/cc-pVQZ level from Ref. [41]; PES-2017: our present work.

The transition state geometric parameters from our *ab initio* calculations and previous works in the literature are shown in Fig. 2. In the previous work, the TS geometry was somewhat uncertain and the corresponding calculations at various *ab initio* levels are not consistent.[13,14] Czako *et al.*[40] described the transition state with the bond lengths being formed (R_{OH}) and broken (R_{CH}) at 2.253 bohr and 2.470 bohr, respectively, and the barrier height of 14.08 kcal/mol. They were

taken as the best estimated values to data and served as benchmark values. The PES-2014 for the title reaction presented the barrier with a height of 14.0 kcal/mol and a lower imaginary frequency for TS of 1900i cm^{-1}, which is much lower than our *ab intio* calculated value of 2376i cm^{-1}. Obviously the thinner barrier obtained in our present work facilitates more facile tunnelling. The barrier height of 14.08 kcal/mol from "benchmark" and 14.0 kcal/mol from "PES-2014" are much higher than the experimental value of 8.7 kcal/mol–11.7 kcal/mol[62] extracted from Arrhenius plots, though Arrhenius expression does not provide a particularly good fit to the experimental data. Our calculated barrier height is 13.55 kcal/mol at the CCSD(T) = FULL/optACVQZ level, in agreement with our previous reported theoretical values.[1,2] An exhaustive geometry optimization for the TS performed at the *ic*MRCI level obtained a similar geometry with $R_{OH} = 2.234$ bohr and $R_{CH} = 2.436$ bohr,[1] but this kind of calculation goes far beyond our currently reasonable computational resources, and neither frequency for TS nor geometry optimizations for other stationary points could be achieved.

In our study, the geometry parameters of Well$_R$ includes $\theta = 0.0°$, $R_{OH} = 6.012$ bohr, $R_{CH} = 2.103$ bohr. The depth of Well$_R$ on PES-2017 is -0.53 kcal/mol , which is much deeper than previous reported values. Therefore, our result indicates that the weakly-bound vdW interaction of the ground-state O atom with methane along the O$\cdots$HCH$_3$ axis is helpful for orienting the system toward Well$_R$. The overall accuracy of the interpolation for the PES-2017 surface is estimated roughly as follows. Two thousand molecular configurations were randomly selected during the integration of trajectories to produce a sample of dynamically relevant geometries. Then *ab initio* calculations at the CCSD(T) = FULL/optACVQZ level are performed at all configurations in this sample, and the error is computed from the difference between the *ab initio* energy and the value obtained from the interpolated surface. The average absolute error is obtained to be 0.60 kcal/mol, and the root-mean-square error is 0.83 kcal/mol.

3.2. Dynamics of the reaction

The full-dimensional QCT calculations with the standard normal-mode sampling for the title reaction are carried out on the newly constructed PES with CH_4 initially in the ground rovibrational state. Two thousand molecular configurations are randomly selected during the integration of trajectories to produce a sample of dynamically relevant geometries. In this step, the initial distance between the center of mass of the reactants is $(x^2 + b^2)^{1/2}$, where b is the impact parameter and $x = 10$ bohr. Then *ab initio* calculations at the CCSD(T) = FULL/optACVQZ level are performed at all configurations in this sample, and the error is computed from the difference between the *ab initio* energy and the value obtained from the interpolated surface. The average absolute error is obtained to be 0.60 kcal/mol, and the root-mean-square error is 0.83 kcal/mol. The initial CH_4 molecule is set in its ground rovibrational state using fixed normal mode energy sampling for all trajectories, and the integration time step is 0.05 fs. The initio rotational angular momentum of the fragments and the impact parameter are set to zero. The maximum value of the impact parameter is estimated by calculating batches of 10^3 trajectories at fixed values of b and systematically increasing the value of the b_{max} until no reactive trajectories are obtained. It should be noted that the QCT calculations are started at the Reactants asymptote with a center of mass separation between the fragments of 30.0 bohr and are stopped when the O–C or one of the C–H internuclear distance reaches 30.0 bohr after the inner turning point of the trajectories.

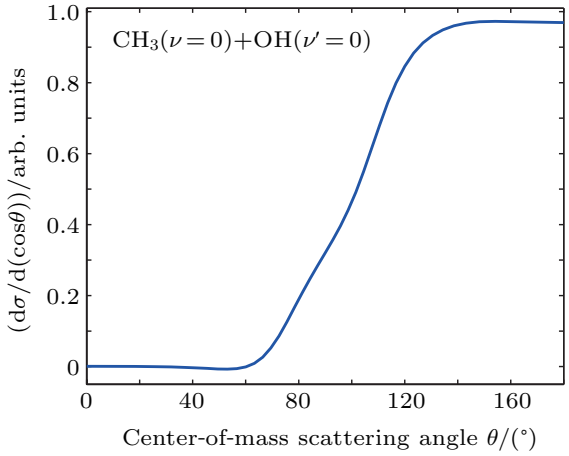


Fig. 3. (color online) Translation energy distribution of products obtained from the QCT calculation.

In the calculations for the reaction probability, the reaction probability from the dynamics calculation was multiplied by a factor of 4 to account for equal and independent contribution to reaction probability from all the hydrogen atoms in CH_4, due to the fact that the hydrogen atom in the reagent CH_4 is treated as distinguishable. Clearly, the reaction probability computed with the classical dynamics is converged to 0.12 with small variations after the reference data set grew to 4500 points. For each energy the maximum value of the impact parameter, b_{max}, was determined by first calculating batches of 10^4 trajectories at fixed values of the impact parameter and then systematically increasing the value of b until no reactive trajectories were obtained. For the title reaction at $E_{col} =$ 30.0 kcal/mol at 300 K, about 5.6×10^5 trajectories have been calculated, which leads to a maximum impact parameter of 5.0 bohr and an average reaction probability of 0.13. An analogous number of trajectories have also been calculated at 100 K, leading to very similar results. The computed angular distributions for the pair-correlated $CH_3(v = 0) + OH(v' = 0)$

products and the center of mass speed distribution $P(E_T)$ obtained by the QCT calculations with $E_{col} = 13.0$ kcal/mol on the newly constructed PES are displayed in Fig. 3 and Fig. 4, respectively. The angular distribution of the OH product in Fig. 3 shows a predominant sharply backward scattering peak relative to the O(^3P) beam direction, where no forward scattering peak or any signal from the sideways scattering is presented. The present angular distribution in our calculation is in accordance with the experimental distribution, which remains confined within the backward hemisphere in the measurements of Liu *et al.*[13,25,26,28,30] The behavior of the center of mass speed distribution indicates that most of the available energy in this reaction is deposited into a particular product mode until the transition state is reached. It could be explained by considering that a larger number of trajectories are removed in the vibrational ground state reaction due to zero point energy violation.[11,43,63] This agrees well with the experimental measurement that about 90% of the total available energy remains as OH co-products rotations.[13,25] The center of mass speed distribution $P(E_T)$ in Fig. 4 obtained by the QCT calculations represents a one-dimensional projection of the desired three-dimensional (3D) state-tagged angular distribution, which can be recovered by the law of cosines.[64] For the product kinetic energy release, only one single peak was found since only the OH products can be formed at the collision energy range in the present work. The normalized differential cross-sections at different collision energies are obtained in Fig. 5, in which a 3D representation shows the evolution of the product-scattering distribution with respect to both scattering angle and collision energy for the reaction of $CH_4 + O(^3P) \rightarrow CH_3(v = 0) + OH(v' = 0)$. Our QCT calculations with different collision energies show that the angular distributions shift toward sideways directions as E_c increases, which is in agreement with the experiments at the common collision energy range 7.0 kcal/mol–15.0 kcal/mol.[13] The behavior of this distribution supports that it is a rebound mechanism, which very closely resembles the experimental results by Liu and his co-workers.[25,26] A 3D polar plot for the product translational energy and angular distributions for the reaction of $CHD_3 + O(^3P) \rightarrow CD_3(v = 0) + OH(v' = 0)$ with $E_{col} = 11.8$ kcal/mol is shown in Fig. 6, indicating that the backward scattering signals are much stronger than those of forward and sideways scattering. Our QCT image for the 3D polar plot is in good agreement with the crossed-beam study for the isotopic product channel, in which the unnormalized raw images for the $CD_3(v = 0)$ products were exemplified with $E_{col} = 11.8$ kcal/mol.[28] All distributions are sharply backward peaking, indicative of a clear direct rebound mechanism. Moreover, the predominant backward scattering peak resides in the high kinetic energy region, which indicates the products stay in their ground vibrational states. From the experimental angular distribution by Liu and his coworkers,[13,28] both images feature a distinct ring-like structure in the backward direction. Our QCT calculations are in good agreement with experimental results after the round-shaped features along the 0-π line were discarded, since they were the beam-generated background noises.

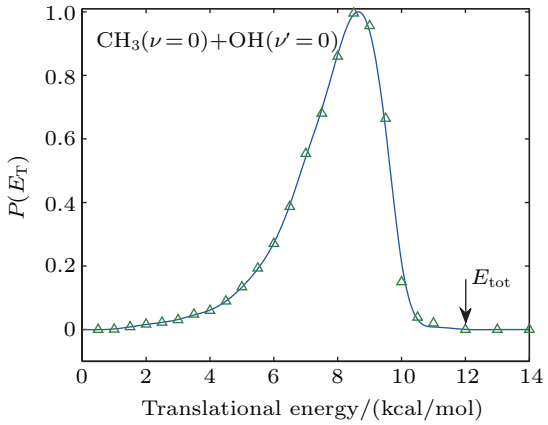


Fig. 4. (color online) Angular distribution of OH($v' = 0$) relative to the direction of the incoming O atom. The forward direction, 0°, is along the initial CH_3 direction in the center-of-mass frame.

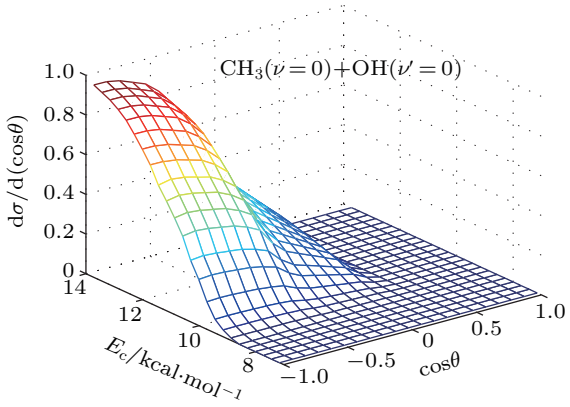


Fig. 5. (color online) Three-dimensional (3D) representation for the evolution of product-scattering distribution with respect to both scattering angle and collision energy for the reaction of CH_4 + O(^3P) → $CH_3(v = 0) + OH(v' = 0)$. The calculations have been performed with E_c energy range 7.0 kcal/mol–15.0 kcal/mol (7.0, 7.9, 9.0, 9.5, 10.0, 10.5, 11.0, 11.5, 11.8, 12.0, 12.4, 13.0, 14.0, 14.2, and 15.0 kcal/mol) in the present work.

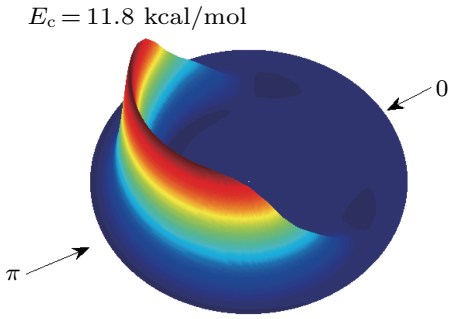


Fig. 6. (color online) Three-dimensional (3D) polar plot for the product translational energy and angular distributions for the reaction of CHD_3 + O(^3P) → $CD_3(v = 0) + OH(v' = 0)$. The forward direction (0) corresponds to the direction of the incoming O atom.

4. Conclusions

In this paper, we presented extensive QCT calculations for the ground-state reaction of $CH_4 + O(^3P) \rightarrow CH_3(v = 0) + OH(v' = 0)$ with the detailed dynamics information performed on a unique full-dimensional *ab initio* PES. The accuracy was achieved by using high-level *ab initio* calculations to compute about 6100 data points with energies and the first and second order derivatives. The modified Shepard interpolation method and the iterative development scheme are employed to construct the interpolated PES. The analysis of properties of our surface shows that it is accurate in important regions and physically reasonable in various regions. QCT computations on this new PES provide a result in good agreement with the experiments and our previous calculations. The rebound mechanism for the title reaction is confirmed by our QCT calculations.

Acknowledgments

The authors thank professor M Collins for providing the GROW2.2 package, and professor M Jordan and Dr. D'Arcy for valuable discussions in the trajectories running on the modified Shepard PES.

References

[1] Peng Y, Jiang Z A and Chen J S 2017 *J. Phys. Chem. A* **121** 2209
[2] Peng Y, Jiang Z A and Chen J S 2018 *Chin. Phys. B* **27** 023401
[3] Zhang L, Luo W L, Ruan W, Jiang G and Zhu Z H 2008 *Chin. Phys. B* **17** 2023
[4] Hou X W, Wan M F and Ma Z Q 2012 *Chin. Phys. B* **21** 103301
[5] Galashev A Y 2013 *Chin. Phys. B* **22** 123602
[6] Li Y L, Suleimanov Y V, Yang M H, Green W H and Guo H 2013 *J. Phys. Chem. Lett.* **4** 48
[7] Liu R, Yang M H, Gábor C, Bowman J M, Li J and Guo H 2012 *J. Phys. Chem. Lett.* **3** 3776
[8] Jiang B and Guo H 2014 *J. Chin. Chem. Soc.* **61** 847
[9] Thanh L N and Stanton J F 2017 *J. Chem. Phys.* **147** 152704
[10] Shao K, Fu B and Zhang D H 2015 *Phys. Chem. Chem. Phys.* **17** 24098
[11] Espinosa-Garcia J, Rangel C and Garcia-Bernaldez J C 2015 *Phys. Chem. Chem. Phys.* **17** 6009
[12] Espinosa-Garcıa J and Garcıa-Bernáldez J C 2000 *Phys. Chem. Chem. Phys.* **2** 2345
[13] Zhang J and Liu K 2011 *Chem. Asian J.* **6** 3132
[14] Yang J Y, Shao K J, Zhang D, Shuai Q A, Fu B, Zhang D H and Yang X M 2014 *J. Phys. Chem. Lett.* **5** 3106
[15] Arezoo D, Nicola S, Lucio C C, Manfred B and Gianaurelio C 2014 *Chem. Phys.* **443** 53
[16] Sweeney G M, Watson A and McKendrick K G 1997 *J. Chem. Phys.* **106** 9172
[17] Ausfelder F, Kelso H and McKendrick K G 2002 *Phys. Chem. Chem. Phys.* **4** 473
[18] Troya D, Schatz G C, Garton D J, Brunsvold A L and Minton T K 2004 *J. Chem. Phys.* **120** 731
[19] Troya D and Garcia-Molina E 2005 *J. Phys. Chem. A* **109** 3015
[20] Garton D J, Minton T K, Troya D, Pascual R and Schatz G C 2003 *J. Phys. Chem. A* **107** 4583
[21] Zhang J M, Lahankar S A, Garton D J, Minton T K, Zhang W Q and Yang X M 2011 *J. Phys. Chem. A* **115** 10894
[22] Suzuki T and Hirota E 1993 *J. Chem. Phys.* **98** 2387
[23] Andresen P and Luntz A C 1980 *J. Chem. Phys.* **72** 5842
[24] Kleinermanns K and Luntz A C 1981 *J. Phys. Chem.* **85** 1966
[25] Wang F and Liu K 2010 *Chem. Sci.* **1** 126
[26] Guo H and Liu K 2016 *Chem. Sci.* **7** 3992
[27] Lin J, Zhou J, Shiu W and Liu K 2003 *Science* **300** 966
[28] Zhang B, Liu K and Czako G 2015 *J. Phys. Chem. A* **119** 7190
[29] Zhang B and Liu K 2005 *J. Phys. Chem. A* **109** 6791
[30] Pan H and Liu K 2014 *J. Chem. Phys.* **140** 191101
[31] Joel M Bowman, Gabor Czako and Fu B 2011 *Phys. Chem. Chem. Phys.* **13** 8094
[32] Fu B, Shan X, Zhang D H and David C Clary 2017 *Chem. Soc. Rev.* **46** 7625
[33] Walch S P and Dunning T H 1980 *J. Chem. Phys.* **72** 3221
[34] Gonzalez C, McDouall J J W and Schlegel H B 1990 *J. Phys. Chem.* **94** 7467
[35] González M, Hernando J, Millán J and Sayós R 1999 *J. Chem. Phys.* **110** 7326
[36] Orlando R N, Francisco M B C and Truhlar D G 1999 *J. Chem. Phys.* **111** 10046.
[37] Shao K, Fu B and Zhang D H 2015 *Chin. J. Chem. Phys.* **28** 403
[38] Corchado J C, Espinosa-Garcıa J, Roberto-Neto O, Chuang Y Y and Truhlar D G 1998 *J. Phys. Chem. A* **102** 4899
[39] Fermin H and Uwe U 2002 *J. Chem. Phys.* **117** 4635
[40] Czakó G and Bowman J M 2012 *Proc. Natl. Acad. Sci. USA* **109** 7997
[41] González-Lavado E, Corchado J C and Espinosa-Garcia J 2014 *J. Chem. Phys.* **140** 064310
[42] Gonźlez-Lavado E, Corchado J C, Suleimanov Y V, Green W H and Espinosa-Garcia J 2014 *J. Phys. Chem. A* **118** 3243
[43] Czakó G 2014 *J. Chem. Phys.* **140** 231102
[44] Zhao H L, Wang W J and Zhao Y 2016 *J. Phys. Chem. A* **120** 7589
[45] Joseph T, Steckler R and Truhlar D G 1987 *J. Chem. Phys.* **87** 7036
[46] Meredith J and Gilbert R 1995 *J. Chem. Phys.* **102** 5669
[47] Martinez R, Enriquez P, Puyuelo M and Gonzalez M 2012 *J. Phys. Chem. A* **116** 5026
[48] Czakó G, Liu R, Yang M, Bowman J M and Guo H 2013 *J. Phys. Chem. A* **117** 6409
[49] Frisch M J, Trucks G W, Schlegel H B, *et al.* 2010 Gaussian 09, Wallingford CT: Gaussian, Inc., see http://www.gaussian.com/
[50] Zheng J J, Zhao Y and Truhlar D G 2009 *J. Chem. Theor. Comput.* **5** 808
[51] Schaefer H F 1998 *Encyclopedia of Computational Chemistry* (London: Jhon Wiley and Sons)
[52] Partridge H and Schwenke D W 1997 *J. Chem. Phys.* **106** 4618
[53] Ma H, Zhang C, Zhang Z, Liu X and Bian W 2012 *Adv. Phys. Chem.* **2012** 236750
[54] Jordan M, Thompson K and Collins M 1995 *J. Chem. Phys.* **102** 5647
[55] Thompson K, Jordan M and Collins M 1998 *J. Chem. Phys.* **108** 8302
[56] Ryan P A 1999 *J. Chem. Phys.* **111** 816
[57] Michael A 2002 *Theor. Chem. Acc.* **108** 313
[58] Ischtwan J and Collins M 1994 *J. Chem. Phys.* **100** 8080
[59] Morris M and Jordan M 2014 *J. Chem. Phys.* **140** 204107
[60] Meredith Jordan, Keiran Thompson, Ryan Bettens, *et al.* GROW, version 2.2, it is a collection of scripts and programs that allow the user to construct molecular potential energy surfaces for either unimolecular/bimolecular reactions or bound-state systems
[61] Crittenden D and Jordan M 2005 *J. Chem. Phys.* **122** 044102
[62] Westenberg A A and de Haas N 1967 *J. Chem. Phys.* **46** 490
[63] Monge-Palacios M, Gonzalez-Lavado E and Espinosa-Garcia J 2014 *J. Chem. Phys.* **141** 094307
[64] Simpson W R, OrrEwing A J, Rakitzis T, Kandel S and Zare R N 1995 *J. Chem. Phys.* **103** 7299